Nanocrystals to Nanorods: A Precursor Approach for the Synthesis of Magnesium Hydroxide Nanorods from Magnesium Oxychloride Nanorods Starting from Nanocrystalline Magnesium Oxide

P. Jeevanandam,[†,‡] R. S. Mulukutla,[§] Z. Yang,[†] H. Kwen,[§] and K. J. Klabunde*[,†]

Department of Chemistry, Kansas State University, 111 Willard Hall, Manhattan, Kansas 66506, and NanoScale Corporation, 1310 Research Drive, Manhattan, Kansas 66502

Received March 9, 2007. Revised Manuscript Received August 4, 2007

Nanorods of magnesium oxychloride ($Mg_x(OH)_yCl_z \cdot nH_2O$) and magnesium hydroxide ($Mg(OH)_2$) have been produced from crystalline MgO. Concentrated aqueous magnesium chloride ($MgCl_2 \cdot 6H_2O$), when allowed to react with MgO, yields oxychloride nanorods that can be converted into $Mg(OH)_2$ nanorods using NaOH, with retention of the nanorod morphologies. A comparison of powdered MgO starting materials has shown that, by proper choice of reagent concentrations, temperature, and aging time, nanorods can be obtained in all cases, but nanocrystalline (NC)−MgO gives the highest yields and the highest aspect ratios (aspect ratios of about 60−90 in the oxychloride system). The higher surface area and higher reactivity of NC−MgO allow the rapid formation of nucleation sites in large numbers that subsequently grow into thin (∼170 nm) oxychloride nanorods. The nanorods of $Mg_x(OH)_yCl_z \cdot nH_2O$ and $Mg(OH)_2$ were characterized by powder X-ray diffraction and transmission electron microscopy measurements.

Introduction

One-dimensional nanostructures such as nanorods, nanowires, and nanotubes are of interest because of their unique optical, electronic, and magnetic properties, and these properties are size and shape dependent.[1−3] The applications of one-dimensional nanostructures include (i) tips in atomic force microscopes,[4] (ii) nanosize electronic devices,[5] (iii) photonic devices,[6] (iv) gas storage and sensing applications,[7] (v) catalysis,[8] (vi) composite materials,[9] and (vii) reinforcing agents.[10] The synthesis methods of one-dimensional nanostructures include using (i) templates,[11] (ii) laser ablation,[12] (iii) chemical vapor deposition,[13] (iv) electrochemical methods,[14] (v) vapor−solid and vapor−liquid−solid mechanisms,[15] and (vi) arc discharge.[16] Examples of the synthesized one-dimensional structures include carbon nanotubes,[17] CaO,[18] MgO,[19] transition metal oxides,[20] WS_2,[21] GaN,[22] gold,[23] etc. Most of these synthetic methods require expensive and sophisticated apparatuses, and solution processing methods have been explored as low cost alternatives.[24,25] Nanorods of semiconductors,[26] metal hydroxides,[27,28] and oxides[29] have

* Corresponding author. E-mail: kenjk@ksu.edu; fax: (785) 532-6666.
† Kansas State University.
‡ Current Address: Department of Chemistry, Indian Institute of Technology Roorkee, Roorkee-247667, India.
§ NanoScale Corporation.

(1) (a) Duan, X.; Huang, Y.; Cui, Y.; Wang, J.; Lieber, C. M. *Nature* **2001**, *409*, 66. (b) Alivisatos, A. P. *Science* **1996**, *271*, 933.
(2) Xia, Y.; Yang, P.; Sun, Y.; Wu, Y.; Mayers, B.; Gates, B.; Yin, Y.; Kim, F.; Yan, H. *Adv. Mater.* **2003**, *15*, 353.
(3) (a) Cui, Y.; Wei, Q. Q.; Park, H. K.; Lieber, C. M. *Science* **2001**, *293*, 1289. (b) Peng, Z. A.; Peng, X. G. *J. Am. Chem. Soc.* **2002**, *124*, 3343. (c) Hu, J. T.; Odom, T. W.; Lieber, C. M. *Acc. Chem. Res.* **1999**, *32*, 435. (d) Peng, X. D.; Manna, L.; Yang, W. D.; Wickham, J.; Scher, E.; Kadavanich, A.; Alivisatos, A. P. *Nature* **2000**, *404*, 59.
(4) Strus, M. C.; Raman, A.; Han, C. S.; Nguyen, C. V. *Nanotechnology* **2005**, *16*, 2482.
(5) (a) Huynh, W. U.; Dittmer, J. J.; Alivisatos, A. P. *Science* **2002**, *295*, 2425. (b) Duan, X.; Huang, Y.; Agarwal, R.; Lieber, C. M. *Nature* **2003**, *421*, 241.
(6) Xi, J. Q.; Kim, J. K.; Schubert, E. F.; Ye, D.; Lu, T. M.; Lin, S. Y.; Juneja, J. S. *Opt. Lett.* **2006**, *31*, 601.
(7) (a) Favier, F.; Walter, E. C.; Zach, M. P.; Benter, T.; Penner, R. M. *Science* **2001**, *293*, 2227. (b) Mohamed, M. B.; Volkov, V.; Link, S.; El-Sayed, M. A. *Chem. Phys. Lett.* **2000**, *317*, 517.
(8) (a) Zhang, W.; Yang, Z.; Wang, X.; Zhang, Y.; Wen, X.; Yang, S. *Catal. Commun.* **2006**, *7*, 408. (b) Fukuoka, A.; Ichikawa, M. *Int. J. Nanosci.* **2005**, *4*, 957.
(9) (a) Kildishev, A.; Cai, W.; Chettiar, U. K.; Yuan, H. K.; Sarychev, A. K.; Drachev, V.; Shalaev, U. M. *J. Opt. Soc. Am. B* **2006**, *23*, 423. (b) Takahashi, K.; Wang, Y.; Lee, K.; Cao, G. *Appl. Phys. A: Mater. Sci. Process.* **2006**, *82*, 27.
(10) Yang, P.; Lieber, C. M. *J. Mater. Res.* **1997**, *12*, 2981.
(11) Dai, H.; Wong, E. W.; Lu, Y. Z.; Fan, S. S.; Lieber, C. M. *Nature* **1995**, *375*, 769.
(12) Hu, J. T.; Odom, T. W.; Lieber, C. M. *Acc. Chem. Res.* **1999**, *32*, 435.
(13) Gao, Y. H.; Bando, Y.; Sato, T.; Zhang, Y. F.; Gao, X. Q. *Appl. Phys. Lett.* **2002**, *81*, 2267.
(14) Ying, Y.; Chang, S. S.; Lee, C. L.; Wang, C. R. C. *J. Phys. Chem. B* **1997**, *101*, 6661.
(15) Yang, P.; Lieber, C. M. *Appl. Phys. Lett.* **1997**, *70*, 3158.
(16) Ijima, S. *Nature* **1991**, *354*, 56.
(17) (a) Archibald, D. D.; Mann, S. *Nature* **1993**, *364*, 430. (b) Chopra, N. G.; Luyken, R. J.; Cherrey, K.; Crespi, V. H.; Cohen, M. L.; Souie, S. G.; Zettle, A. *Science* **1995**, *269*, 966.
(18) Xu, X. L.; Yu, D. P.; Feng, S. Q.; Duan, X. F.; Zhang, Z. *Nanostruct. Mater.* **1997**, *8*, 373.
(19) (a) Wei, Q.; Lieber, C. M. *Mater. Res. Soc. Symp. Proc.* **2000**, *581*, 3. (b) High-purity fibrous basic magnesium chloride. Sumitomo Chemical Co., Jpn Kokai Tokkyo Koho, 1985, JP60021813.
(20) Seo, J.; Jun, Y.; Ko, S. J.; Cheon, J. J. *Phys. Chem. B* **2005**, *109*, 5389.
(21) Tenne, R.; Margulis, L.; Genut, M.; Hodes, G. *Nature* **1992**, *360*, 444.
(22) Han, W. Q.; Fan, S. S.; Li, Q. Q.; Hu, Y. D. *Science* **1997**, *277*, 1287.
(23) Gole, A.; Murphy, C. J. *Chem. Mater.* **2005**, *17*, 1325.
(24) (a) Li, M.; Schnableggar, H.; Mann, S. *Nature* **1999**, *402*, 393. (b) Tang, Z. Y.; Kotov, N. A.; Giersig, M. *Science* **2002**, *297*, 237. (c) Holmes, J. D.; Johnston, K. P.; Doty, R. C.; Korgel, B. A. *Science* **2000**, *287*, 1471.
(25) (a) Vayssieres, L. *Adv. Mater.* **2003**, *15*, 464. (b) Wang, W.; Bai, F. *Chem. Phys. Commun.* **2003**, *4*, 761. (c) Wang, W. S.; Xu, C. Y.; Zhen, L.; Yang, L.; Shao, W. Z. *Chem. Lett.* **2006**, *35*, 268.

10.1021/cm070666t CCC: $37.00
Published on Web 09/29/2007

been synthesized by solution based synthetic methods. There is ongoing research to devise simpler, larger scale methods to synthesize nanorods.

Magnesium oxychlorides ($Mg_x(OH)_yCl_z.nH_2O$), also known as Sorel cement, were discovered in 1867.[30] They possess interesting properties such as a low thermal conductivity, high fire retardancy, and good mechanical, acoustic, and elastic properties.[31−33] $Mg_x(OH)_yCl_z{\cdot}nH_2O$ are useful in thermal barrier coatings,[34] as flame and smoke retardants, as fire resistant coatings,[35,36] and as cement and packing materials.[37] Likewise, and of close relevance to the current work, $Mg_x(OH)_yCl_z{\cdot}nH_2O$ (e.g., $Mg_2(OH)_3Cl{\cdot}4H_2O$) have been used as precursors to produce nanorods of $Mg(OH)_2$ and magnesium oxide (MgO).[19] $Mg_x(OH)_yCl_z{\cdot}nH_2O$ possess a needle-like structure, and they are synthesized from aqueous concentrated solutions of magnesium chloride and MgO. $Mg_x(OH)_yCl_z{\cdot}nH_2O$ are formed only at higher concentrations of magnesium chloride (e.g., 3 M or more), while at lower concentrations, only the formation of $Mg(OH)_2$ occurs. The consumption of MgO is faster in the presence of magnesium chloride, and four different $Mg_x(OH)_yCl_z{\cdot}nH_2O$ phases have been reported[38] depending on the concentration of the reagents and temperature: (i) $5Mg(OH)_2{\cdot}MgCl_2{\cdot}8H_2O$ (phase 5), (ii) $3Mg(OH)_2{\cdot}MgCl_2{\cdot}8H_2O$ (phase 3), (iii) $2Mg(OH)_2{\cdot}MgCl_2{\cdot}5H_2O$ (phase 2), and (iv) $9Mg(OH)_2{\cdot}MgCl_2{\cdot}6H_2O$ (phase 9). Phases 5 and 3 are obtained at temperatures below 100 °C; phase 5 transforms to phase 3 if there is excess $MgCl_2$. Phases 2 and 9 are obtained at temperatures above 100 °C.

Crystals and nanorods of $Mg(OH)_2$ (brucite) and MgO are very important materials. MgO, in general, is used in catalysis supports, ceramic industries, pharmaceutical industries, etc.[39] MgO nanorods are reported to be useful as novel catalytic materials and also as reinforcing agents in composites.[40] MgO nanorods have been used as pinning centers in superconductors, and materials with large critical current densities have been reported.[41] $Mg(OH)_2$ nanorods are usually employed as the precursor for the MgO nanorods,[19] and the synthesis of $Mg(OH)_2$ nanorods is very important. The various synthetic approaches reported in the literature for the synthesis of $Mg(OH)_2$ nanorods is described next.

Lieber and Wei have reported a solution based approach for the synthesis of $Mg(OH)_2$ nanorods (length: ≥10 μm and diameter: 40−200 nm) starting from magnesium chloride and MgO.[19a] Fan et al. have reported the synthesis of $Mg(OH)_2$ nanorods and nanotubes via a solvothermal synthetic route; the nanorods (length: several micrometers and diameter: 200 nm) were obtained when pyridine was used as the solvent at 180 °C.[42] Using a solvothermal process, Li et al. have synthesized $Mg(OH)_2$ nanorods (length: 200−400 nm and diameter: 8−20 nm) from magnesium powder, water, and ethylenediamine.[43] $Mg(OH)_2$ nanorods with a length of ∼3 μm and diameter of ∼30 nm have been prepared by Yan et al. by the hydrolysis of magnesium sulfate in aqueous NH_4OH under hydrothermal conditions.[44] The preparation of $Mg(OH)_2$ nanorods (length: >250 nm and diameter: 8−10 nm) by a liquid−solid arc discharge method has been reported by Hao et al.[45] Rod-like nanoparticles of $Mg(OH)_2$ (length: 4 μm and diameter: 95 nm) have been synthesized by Lu et al. using homogeneous precipitation.[46] Among the reported synthetic methods for $Mg(OH)_2$ nanorods, only the method used by Lieber et al. produces $Mg(OH)_2$ nanorods with high aspect ratios (50 or higher).[19a,41] In this method, $Mg_x(OH)_yCl_z{\cdot}nH_2O$ has been used as a precursor for the synthesis of $Mg(OH)_2$ and MgO nanorods; the morphology of the precursor rods is retained during its conversion to $Mg(OH)_2$ and MgO nanorods. Sorrell and Armstrong[47] have reported that the morphology of MgO has a significant effect on the formation of $Mg_x(OH)_yCl_z{\cdot}nH_2O$. With the availability of a variety of crystalline forms of MgO with enhanced reactivity,[48] the goal of the present work was to determine if a larger scale, more efficient synthesis of high aspect ratio nanorods of $Mg_x(OH)_yCl_z{\cdot}nH_2O$ and $Mg(OH)_2$ could be achieved.

Experimental Procedures

The synthesis of $Mg_x(OH)_yCl_z{\cdot}nH_2O$ rods was based on the work performed by Wei and Lieber.[19a] The effect of using nanocrystalline (NC)−MgO instead of macrocrystalline (MC)−MgO during the synthesis has been investigated, and the synthesis was carried out, under similar conditions, using three different MgOs; two types of

(26) (a) Manna, L.; Milliron, D. J.; Meisel, A.; Scher, E. C.; Alivisatos, A. P. *Nat. Mater.* **2003**, *2*, 382. (b) Lee, S. M.; Jun, Y.; Cho, S. N.; Cheon, J. *J. Am. Ceram. Soc.* **2002**, *124*, 11244.
(27) Kuiry, S. C.; Megen, E.; Patil, S. D.; Deshpande, S. A.; Seal, S. *J. Phys. Chem. B* **2005**, *109*, 3868.
(28) Fan, W.; Sun, S.; Song, X.; Zhang, W.; Yu, H.; Tan, X.; Cao, G. *J. Solid State Chem.* **2004**, *177*, 2329.
(29) Lu, C.; Qi, L.; Zhang, D.; Wu, N.; Ma, J. *J. Phys. Chem. B* **2004**, 108, 17825.30.
(30) Sorel, S. *Comp. Rend.* **1867**, *65*, 102.
(31) (a) Montle, J. F.; Mayhan, K. G. *J. Fire Flammability/Fire Retard. Chem. Suppl.* **1974**, *1*, 243. (b) Montle, J. F.; Mayhan, K. G. *Loss Prevention* **1974**, *8*, 52.
(32) Schwab, R. F.; Lawler, J. B. *Loss Prevention* **1974**, *8*, 42.
(33) Montle, J. F.; Mayhan, K. G. *Fire Technol.* **1974**, *10*, 21.
(34) duPont de Nemours; Stewart, C. W. Fire-resistant polymers containing magnesium oxychloride. U.S. Patent 4,772,654, 1988.
(35) Herrera, M. E. *ASTM Spec. Tech. Publ.* **1983**, *826*, 94.
(36) Kawaller, S. I. *Fire Technol.* **1977**, *13*, 139.
(37) Policastro, P. P.; Tarneja, R. S. Fire-resistant and long pot-life zinc containing magnesium oxychloride cement. U.S. Patent 5,039,454, 1991.
(38) (a) Sorrell, C. A.; Armstrong, C. R. *J. Am. Ceram. Soc.* **1976**, *59*, 51. (b) Matkovic, B.; Popovic, S.; Rogic, V.; Zunic, T.; Young, J. F. *J. Am. Chem. Soc.* **1977**, *60*, 504. (c) Christensen, A. N.; Norby, P.; Hanson, J. C. *Acta Chem. Scand.* **1995**, *49*, 331. (d) Bilinski, H.; Matkovic, B.; Mazuranic, C.; Zunic, T. B. *J. Am. Ceram. Soc.* **1984**, *67*, 266. (e) Christensen, A. N. *Mater. Res. Soc. Symp. Proc.* **1992**, *205*, 259.
(39) Tsuji, H.; Yagi, Y.; Hattori, H.; Kita, H. *J. Catal.* **1994**, *148*, 759.
(40) (a) Soylu, B.; Adamopoulos, N.; Glowacka, D. M.; Evetts, J. E. *Appl. Phys. Lett.* **1992**, *60*, 22. (b) Driessen, J. M.; Poels, E. K.; Hinderman, J. P.; Ponec, V. *J. Catal.* **1983**, *82*, 26. (c) Znaidi, L.; Chhor, K.; Pommier, C. *Mater. Res. Bull.* **1996**, *31*, 1527.
(41) Yang, P.; Lieber, C. M. *Science* **1996**, *273*, 1836.
(42) Fan, W.; Sun, S.; Song, X.; Zhang, W.; Yu, H.; Tan, X.; Cao, G. *J. Solid State Chem.* **2004**, *177*, 2329.
(43) Li, Y.; Sui, M.; Ding, Y.; Zhang, G.; Zhuang, J.; Wang, C. *Adv. Mater.* **2000**, *12*, 818.
(44) Yan, L.; Zhuang, J.; Sun, X.; Deng, Z.; Li, Y. *Mater. Chem. Phys.* **2002**, *76*, 119.
(45) Hao, L.; Zhu, C.; Mo, X.; Jiang, W.; Hu, Y.; Zhu, Y.; Chen, Z. *Inorg. Chem. Commun.* **2003**, *6*, 229.
(46) Lu, J.; Qiu, L.; Qu, B. *Nanotechnology* **2004**, *15*, 1576.
(47) Sorrell, C. A.; Armstrong, C. R. *J. Am. Ceram. Soc.* **1976**, *59*, 51.
(48) (a) Klabunde, K. J.; Stark, J. V.; Koper, O.; Mohs, C.; Park, D. G.; Decker, S.; Jiang, Y.; Lagadic, I.; Zhang, D. *J. Phys. Chem.* **1996**, *100*, 12142. (b) Lucas, E.; Decker, S.; Khaleel, A.; Seitz, A.; Fultz, S.; Ponce, A.; Li, W.; Carnes, C.; Klabunde, K. J. *Chem.−Eur. J.* **2001**, *7*, 2505.

Table 1. Synthesis of Mg$_x$(OH)$_y$Cl$_z$·*n*H$_2$O: Preliminary Experimental Conditions for Scale-Up Using MC−MgO

expt no.	MgO (g)	$MgCl_2·6H_2O$ (g)	water (mL)	stirring time (h)	length (μm)	width (μm)
A	4.0	27.12	48	8.0	ND[a]	ND
B	4.0	40.68	48	1.5	4.1 ± 1.6	0.3 ± 0.1
C	4.0	54.24	48	2.0	8.5 ± 4.4	0.9 ± 0.6
D	4.0	67.80	48	3.3	7.2 ± 2.6	0.5 ± 0.2
E	4.0	81.36	48	4.0	6.9 ± 3.4	0.5 ± 0.2
F	4.0	135.60	48	6.5	4.5 ± 2.4	0.3 ± 0.1

[a] ND: not determined.

NC−MgO and a MC−MgO. The NC−MgO, NanoActive MgO (crystallite size: ≤8nm and surface area: ≥230 m^2/g) and NanoActive MgO Plus (crystallite size: ≤4nm and surface area: ≥600 m^2/g), were received from NanoScale Corporation, Manhattan, KS and were used as received. These two NC−MgOs will henceforth be referred to as NC−MgO−I −(crystallite size: ≤8nm) and −NC−MgO−II (crystallite size: ≤4nm), respectively. $MgCl_2·6H_2O$ was received from Fisher Scientific and the MC (bulk) MgO (MC−MgO) was received from Aldrich (−325 mesh); the measured BET surface area (by nitrogen adsorption using a NOVA 1000 instrument from Quantachrome) for this oxide was about 45 m^2/g, and the Debye−Scherrer crystallite size was about 23 nm. Mg$_x$(OH)$_y$Cl$_z$·*n*H$_2$O was synthesized first, and the details of the synthesis of Mg$_x$(OH)$_y$Cl$_z$·*n*H$_2$O are as follows.

Small Scale Syntheses. A total of 75 (±0.5) g of $MgCl_2·6H_2O$ was diluted to 125 mL in a 250 mL Erlenmeyer flask using deionized water. A total of 0.45 (±0.01) g of MgO (NC−MgO−I, NC−MgO−II, or MC−MgO) was added slowly with stirring, at 25 °C, in about 20 min in equal portions ([MgO]/[$MgCl_2$] = 0.03). After about 1 h and 30 min, a clear solution resulted in the case of NC−MgO−II, but cloudy solutions were noticed in the case of the other two oxides (i.e., NC−MgO−I and MC−MgO). The contents were stirred for about 21 h (aging step) at four different temperatures (25, 40, 50, or 70 °C). The contents were centrifuged and washed with water (at least 4 times) and finally with alcohol. When NC−MgO−II (crystallite size: ≤4 nm) was used, slightly viscous slurries were obtained at 25 and 40 °C aging temperatures, while at 50 and 70 °C aging temperatures, gels were obtained. On the other hand, fluffy precipitates were obtained in the case of NC−MgO−I (crystallite size: ≤8 nm), and MC−MgO at all the aging temperatures (25, 40, 50, and 70 °C). The yield of the syntheses using this procedure was dependent on the starting MgO added, aging time, and stirring speed and was usually about 1 g.

Large Scale Syntheses. To increase the yield of precursor nanorods from one batch, the following preliminary experiments were performed. Instead of using 0.45 g of MgO, about 4 g of MgO (Aldrich, −325 mesh) was mixed into about 48 mL of aqueous solution dissolved with different amounts of $MgCl_2·6H_2O$ (stirring speed: 300 rpm). The various experimental conditions and the amount of starting materials used are listed in Table 1. For experiment A, the stirring was turned off manually after 8 h. For experiments B−F, stirring stopped naturally when the suspensions became slurries that were too thick to be stirred anymore. After the stirring stopped, all the samples were aged at room temperature (∼25 °C) on the bench (sealed by a rubber stopper) up to 72 h after the addition of MgO. The samples were washed with water and ethanol and then used for TEM and XRD analysis. Conditions C and D were found to be the optimum conditions, and about 10 g of Mg$_x$(OH)$_y$Cl$_z$·*n*H$_2$O was produced.

Conversion to Mg(OH)$_2$ Nanorods. The Mg$_x$(OH)$_y$Cl$_z$·*n*H$_2$O nanorods were converted into the Mg(OH)$_2$ phase by NaOH treatment at various temperatures (25−70 °C) and concentrations (1−6M) in ethanol water solutions (3:1) for various time periods (3−19 h). In a typical experiment, about 3 g of the precursor slurry, after washing with water and ethanol, was added to the desired NaOH solution (100 mL prepared using 3:1 EtOH-H_2O or H_2O alone), heated to the desired temperature, and stirred at this temperature for a particular time period. After the NaOH treatment, the contents were centrifuged, washed with water repeatedly, washed with alcohol, and finally dried in the drying cabinet.

Characterization. The phase analysis for the materials was carried out using a powder X-ray diffractometer (Bruker Advance D8, wavelength: 1.5406 Å). The slurries of the samples in ethanol were used to prepare glass slides for the diffraction measurements, and the slides were dried in air. The TEM examinations of the samples were carried out using a Philips EM100 microscope operating at an accelerating voltage of 100 kV. The slurries of the samples in ethanol were sonicated for about 2 min, and a few drops

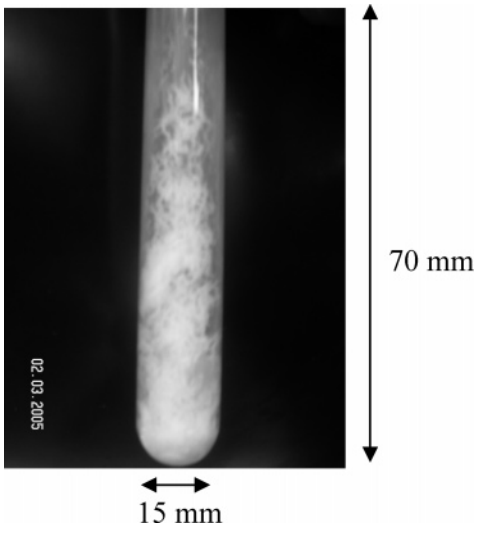

Figure 1. Typical photographic image of Mg$_x$(OH)$_y$Cl$_z$·*n*H$_2$O synthesized.

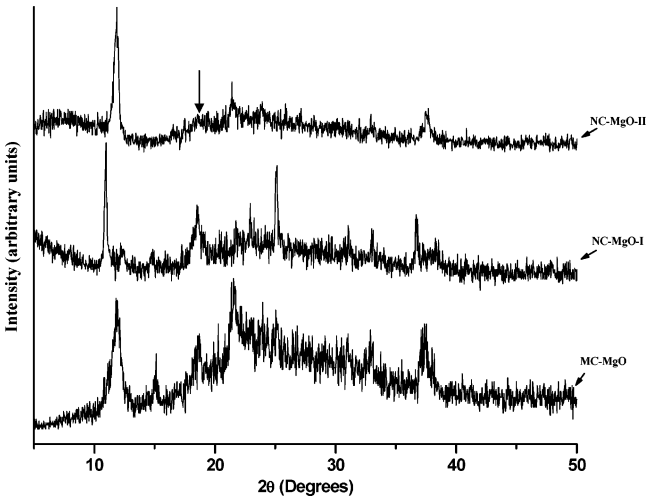

Figure 2. XRD patterns of Mg$_x$(OH)$_y$Cl$_z$·*n*H$_2$O synthesized using three different MgOs at 25 °C (aging time: ∼21 h). Mg(OH)$_2$ appears as an impurity (indicated by an arrow) in some cases; NC−MgO−I and MC−MgO are also shown.

Table 2. Comparison of Products Obtained during Synthesis of $Mg_x(OH)_yCl_z{\cdot}nH_2O$ Using Three Different MgOs[a]

MgO used	aging at 25 °C	aging at 40 °C	aging at 50 °C	aging at 70 °C
NC−MgO−II	precipitate ($Mg_3(OH)_5Cl{\cdot}4H_2O$)	precipitate ($Mg_3(OH)_5Cl{\cdot}4H_2O$)	gel	gel
NC−MgO−I	precipitate ($Mg_2(OH)_3Cl{\cdot}4H_2O$) + $Mg(OH)_2$	precipitate ($Mg_2(OH)_3Cl{\cdot}4H_2O$)	precipitate ($Mg_2(OH)_3Cl{\cdot}4H_2O$)	precipitate ($Mg_2(OH)_3Cl{\cdot}4H_2O$)
MC−MgO	precipitate ($Mg_3(OH)_5Cl{\cdot}4H_2O$) + $Mg(OH)_2$	precipitate ($Mg_2(OH)_3Cl{\cdot}4H_2O$)	precipitate ($Mg_2(OH)_3Cl{\cdot}4H_2O$)	precipitate ($Mg_2(OH)_3Cl{\cdot}4H_2O$)

[a] Aging time: ∼21 h.

of the solutions were allowed to dry in air on Formvar coated copper grids (300 mesh from Electron Microscopic Sciences).

Results and Discussion

A photographic image of the $Mg_x(OH)_yCl_z{\cdot}nH_2O$, synthesized in the present study, is shown in Figure 1. The fibrous nature of the material can be clearly seen. The typical XRD patterns for the products obtained during the synthesis of $Mg_x(OH)_yCl_z{\cdot}nH_2O$ are shown in Figure 2. The products obtained depend on the aging temperature as well as the nature of MgO used. The products obtained using three different MgOs (NC−MgO−I, NC−MgO−II, and MC−MgO) were analyzed by powder XRD measurements, and the results are summarized in Table 2. In most cases, the observed pattern matches with that of $Mg_2(OH)_3Cl{\cdot}4H_2O$ (JCPDS file 7−412), the one reported by Lieber and Wei.[19a] When NC−MgO−II was used, the products were gels at 70 and 50 °C aging temperatures; attempts to dry the gels either by vacuum or inside a drying cabinet (temperature: ∼80 °C) resulted in decomposition of the gels to $MgCl_2{\cdot}6H_2O$ (JCPDS file 77−1268). At 40 and 25 °C aging temperatures, on the other hand, the products were crystalline ($Mg_2(OH)_3Cl{\cdot}4H_2O$ or $Mg_3(OH)_5Cl{\cdot}4H_2O$ (JCPDS file 7−409)). When NC−MgO−I was used, all four aging temperatures (25, 40, 50, and 70 °C) yielded crystalline $Mg_2(OH)_3Cl{\cdot}4H_2O$. When MC−MgO was used, crystalline $Mg_2(OH)_3Cl{\cdot}4H_2O$ was the product at all four aging temperatures. However, for the product synthesized at the 70 °C aging temperature, in addition to the peaks due to $Mg_2(OH)_3Cl{\cdot}4H_2O$, prominent peaks due to $MgCl_2{\cdot}6H_2O$ were also observed; the decomposition of $Mg_x(OH)_yCl_z{\cdot}nH_2O$ is attributed to the formation of $MgCl_2{\cdot}6H_2O$ in this case.

The TEM images of the products, prepared using three different MgOs at different aging temperatures, are shown in Figure 3a−c. A summary of TEM observations for the products is given in Table 3. When NC−MgO−II (crystallite size: ≤4 nm) was used, 70 and 50 °C aging temperatures produced longer rods (≥20 μm) as compared to the 40 and 25 °C cases (length: ∼4−16 μm). The $Mg_x(OH)_yCl_z{\cdot}nH_2O$ nanorods prepared at 50 and 40 °C aging temperatures are uniform in size (the width of $Mg_x(OH)_yCl_z{\cdot}nH_2O$ was about 170 nm) when compared to the nanorods prepared with the other two aging temperatures (25 and 70 °C).

When NC−MgO−I was used during the synthesis, the morphology of the oxychloride nanorods was different (Figure 3b). At 25 °C aging, the formation of the rods was incomplete. At higher aging temperatures (40−70 °C), the rods were formed, but they look hollow in some places. The length of the rods varied from about 7−15 μm, and the width varied from about 0.1−0.4 μm. Using MC−MgO also produces $Mg_x(OH)_yCl_z{\cdot}nH_2O$ nanorods with different morphologies (Figure 3c). At 70 °C, the rods look deformed, but at 50 and 40 °C, rods with lengths of the order of a few micrometers (∼2−6 μm) could be seen. At 25 °C aging, the formation of the rods is incomplete, although some rods could be seen. Among the three different MgOs (NC−MgO−I, NC−MgO−II, and MC−MgO) investigated during the synthesis of $Mg_x(OH)_yCl_z{\cdot}nH_2O$, NC−MgO−II yields the longest rods (20 μm or longer). For $Mg_x(OH)_yCl_z{\cdot}nH_2O$ prepared at the same aging temperature (e.g., 50 °C), the length of the rods obtained using NC−MgO−II or NC−MgO−I was longer as compared to those obtained using MC−MgO. Also, the diameter of the $Mg_x(OH)_yCl_z{\cdot}nH_2O$ nanorods obtained from NC−MgO−II was smaller (∼170 nm) when compared to that obtained using NC−MgO−I or MC−MgO (∼0.1−0.4 μm). Under the same conditions (temperature: ∼25 °C and aging time: ∼21 h), the formation of the oxychloride rods was complete only if NC−MgO−II was used (Figure 4); if MC−MgO was used, the formation of the rods was not complete. Using NC−MgO−I yielded $Mg_x(OH)_yCl_z{\cdot}nH_2O$ rods, but the rods were only in the process of formation. The TEM results shown in Figure 4 were corroborated by the XRD results. $Mg(OH)_2$ appeared as an impurity if MC−MgO or NC−MgO−I was used during the synthesis (see Figure 2). The individual rods are not single crystals but an amalgamation of nanocrystals. If they were single crystals, then the XRD should show extremely sharp peaks since their width is about 100 nm (large for a crystalline metal oxide).

Since using nanocrystalline MgO produced oxychloride nanorods with a higher aspect ratio, the synthetic conditions were further optimized with respect to the effect of aging time (15−72 h) and stirring speed (150−400 rpm) at room temperature (∼25 °C). The products were analyzed by XRD and TEM measurements, and the results are summarized in Table 4. The important findings of the optimization studies are (i) the yield increases as a function of aging time (Table 4a), keeping the temperature and stirring speed constant (∼25 °C and 300 rpm, respectively), (ii) under the same aging time (∼48 h) and temperature (∼25 °C), a lower stirring speed (150 rpm) affects the phase formed as well as the yield (Table 4b), and (iii) higher stirring speeds (300 and 450 rpm) affect only the yield, and the same phase ($Mg_3(OH)_5Cl{\cdot}4H_2O$) is formed (Table 4b). The present synthetic method produced $Mg_x(OH)_yCl_z{\cdot}nH_2O$ nanorods (∼0.6 g) in about 20 h, if NC−MgO was used. On the other hand, if MC−MgO was used, only a mixture (∼0.8 g) of $Mg(OH)_2$ and $Mg_x(OH)_yCl_z{\cdot}nH_2O$ was obtained in ∼20 h; it takes about 48 h for the complete formation of $Mg_x(OH)_yCl_z{\cdot}nH_2O$. A longer aging time leads to thicker rods (∼0.24−0.56 μm in 72 h), while the faster method leads to thinner rods (∼0.15−0.38 μm in 21 h). The aspect ratio (length/width) was calculated from the averaging of length and width

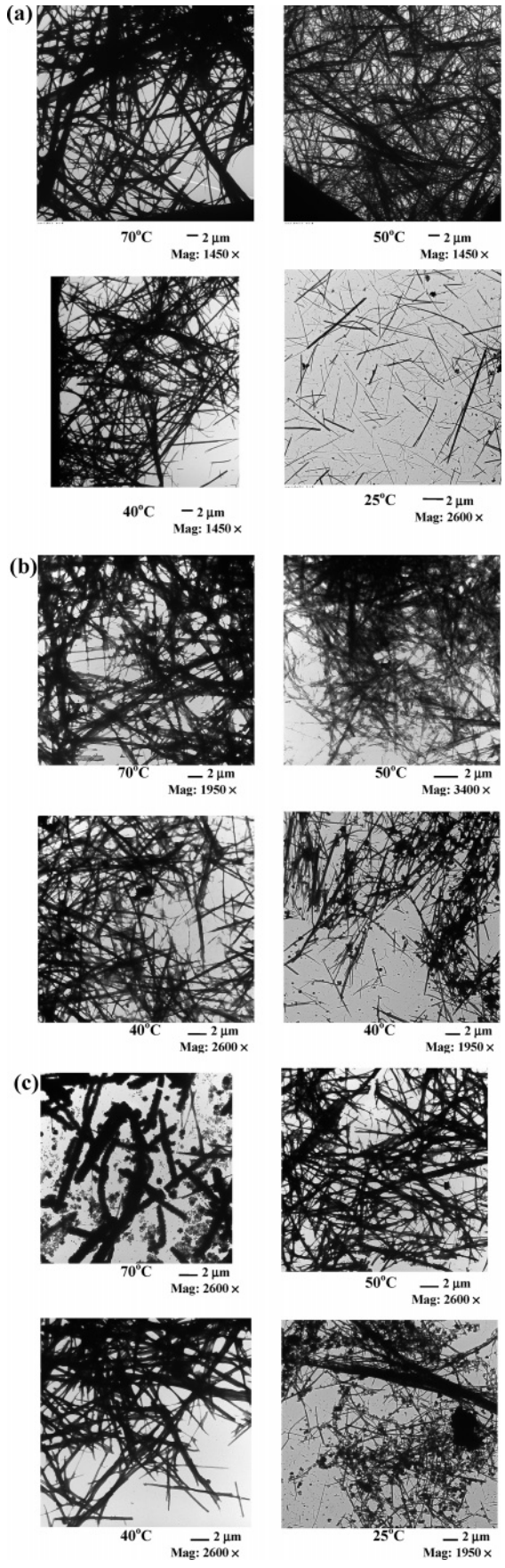

Figure 3. (a) TEM images of the Mg$_x$(OH)$_y$Cl$_z$·nH$_2$O synthesized using NC−MgO−II at different aging temperatures. (b) TEM images of products synthesized using NC−MgO−I at different aging temperatures. (c) TEM images of products synthesized using MC−MgO at different aging temperatures.

measurements of the oxychloride nanorods from TEM images. Figure 5 illustrates the typical aspect ratio distribution plots. The plots show the frequency (number of rods) as a function of length, width, and aspect ratio calculated from the length and width of the rods. The results of aspect ratio calculations in the form of mean values for various optimized synthetic conditions are summarized in Table 4c. The important findings from aspect ratio calculations are (i) the mean length and mean width of the oxychloride nanorods increase as a function of aging time at constant stirring (e.g., 300 rpm), (ii) under a constant aging time (48 h), increasing the stirring speed (300−450 rpm) results in rods with a lower mean length and width, and (iii) the mean aspect ratio of the oxychloride nanorods is about the same ($\sim 45 \pm 25$) for all the conditions; the exception is, under 21 h aging with a stirring speed 300 rpm, the aspect ratio is slightly high, $\sim 55 \pm 31$.

Different mechanisms for the formation of Mg$_x$(OH)$_y$Cl$_z$·nH$_2$O have been discussed in the literature, although they are far from clear. According to Bilinski et al.,[49] the concentration of the total magnesium and chloride ions and the pH of the solution determine the reaction products. The role of MgO is to increase the total concentration of magnesium ions and also to increase the pH of the $MgCl_2$ solution. According to Ved et al.,[50] phases 3 and 5 ($Mg_2(OH)_3Cl{\cdot}4H_2O$) and $Mg_3(OH)_5Cl{\cdot}4H_2O$, respectively) form through ions such as $[HO-Mg-O]^-$, $[Mg(H_2O)_{6-x}{\cdot}Cl]^+$, $[Mg(H_2O)_{6-x}{\cdot}OH]^+$, OH^-, Cl^-, H^+, and $[Mg(OH)]^+$ and not through $Mg(OH)_2$ and $MgCl_2$.[50] Another widely accepted mechanism for the formation of Mg$_x$(OH)$_y$Cl$_z$·nH$_2$O is that first a complex ion such as $[Mg_x(OH)_y(H_2O)_z]_{2x-y}$ forms, along with Cl^-,OH^-, and this reacts with $Mg(OH)_2$ to produce amorphous oxychloride, which slowly crystallizes; when the complex ion is formed, it effectively removes the magnesium ions from solution, subsequently changing its pH.[51]

To gain further information on the formation mechanism of Mg$_x$(OH)$_y$Cl$_z$·nH$_2$O, the synthesis was carried out using four different nanocrystalline oxides (ZnO, Al_2O_3, CeO_2, and TiO_2, marketed as NanoActive oxides by the NanoScale Corporation[52]) instead of NC−MgO, keeping all the other conditions the same (see Experimental Procedures). These experiments were carried out to find out whether the role of MgO is simply to supply the seed crystals for the further growth of Mg$_x$(OH)$_y$Cl$_z$·nH$_2$O rods. If it is so, any NC metal oxide should be able to supply the seed crystals for the further growth of rods. All four nanocrystalline oxides studied (ZnO, Al_2O_3, CeO_2, and TiO_2) did not lead to the formation of Mg$_x$(OH)$_y$Cl$_z$·nH$_2$O; in each case, only the starting oxide material or its hydrolysis product was observed by XRD analysis. These experiments suggest that MgO is required for the formation of Mg$_x$(OH)$_y$Cl$_z$·nH$_2$O rods and that other nanosized oxides do not facilitate their formation. NC−MgOs

(49) Bilinski, H.; Matkovic, B.; Mazuranic, C.; Zunic, T. B. *J. Am. Ceram. Soc.* **1984**, *67*, 266.
(50) Ved, E. I.; Zharov, E. F.; Phong, H. V. *Zh. Prikl. Khim.* **1976**, *49*, 2154.
(51) Dehua, D.; Chuanmei, Z. *Cem. Concr. Res.* **1999**, *29*, 1365.
(52) Crystallite size, surface area, and other characteristics of the nanocrystalline oxides can be downloaded from http://www.nanoscalecorp.com/products_and_services.

Table 3. TEM Observations of $Mg_x(OH)_yCl_z \cdot nH_2O$ Obtained at Different Aging Temperatures[a]

MgO used[b]	aging temp (°C)	dimension (from TEM) (μm)	comment
NC−MgO−II	25, 40	length: ∼4−16	
	50, 70	length: ≥20	
		width: ∼0.17	
NC−MgO−I	25		incomplete formation of rods
	40, 50, 70	length: ∼7−15	
		width: ∼0.1−4	
MC−MgO	25		incomplete formation of rods
	40, 50	length: ∼2−6	
		width: ∼0.1−4	
	70		decomposed rods

[a] Aging time: ∼21 h. [b] NC−MgO−II: nanocrystalline MgO (crystallite size ≤4 nm); NC−MgO−I: nanocrystalline MgO (crystallite size ≤8 nm); and MC−MgO: macrocrystalline MgO (crystallite size ∼23 nm)

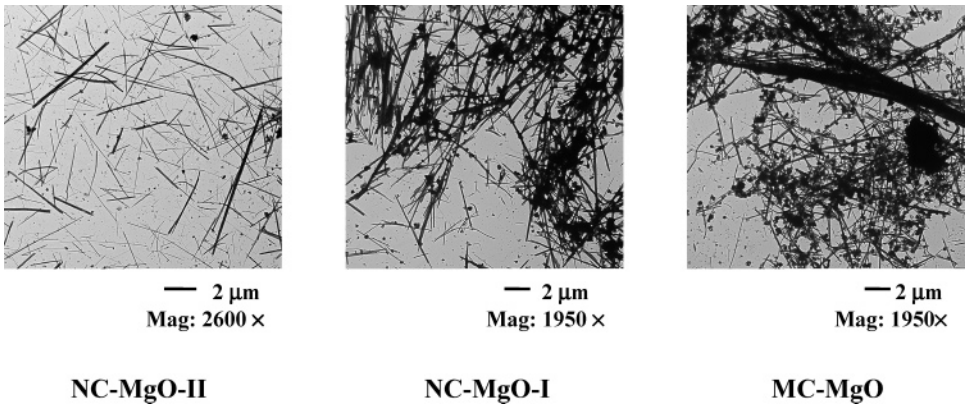

Figure 4. TEM images of products obtained at 25 °C aging for about 21 h, using NC−MgO−II, NC−MgO−I, and MC−MgO.

Table 4. (a) Synthesis of $Mg_x(OH)_yCl_z \cdot nH_2O$ from NC−MgO−II with Different Aging Times, (b) Effect of Stirring Rate on Synthesis of $Mg_x(OH)_yCl_z \cdot nH_2O$,[a] and (c) Calculated mean for Aspect Ratio, Length, and Width of $Mg_3(OH)_5Cl \cdot 4H_2O$ Nanorods Prepared at Different Aging Times and Stirring Speeds

(a) aging time (h)	yield (g)	XRD	TEM results (μm)	aspect ratio range
15	∼0.2	predominant peaks for $Mg_3(OH)_5Cl \cdot 4H_2O$ and significant amount of $Mg(OH)_2$	length: ∼9−16 width: ∼0.2−0.5	∼19−50
21	∼0.6	predominant peaks for $Mg_3(OH)_5Cl \cdot 4H_2O$ and insignificant amount of $Mg(OH)_2$	length: ∼1.5−17.0 width: ∼0.15−0.38	∼10−45
48	∼0.9	predominant peaks for $Mg_3(OH)_5Cl \cdot 4H_2O$ and insignificant amount of $Mg(OH)_2$	length: ∼8−17 width: ∼0.15−0.5	∼15−87
72	∼2.4	predominant peaks for $Mg_3(OH)_5Cl \cdot 4H_2O$	length: ∼4.5−23.5 width: ∼0.24−0.56	∼16−60

			TEM		
(b) stirring rate (rpm)	yield (g)	XRD (phase)	length (μm) range	width (μm) range	aspect ratio range
150	∼0.2	$Mg(OH)_2$	ND[b]	ND	ND
300	∼0.9	$Mg_3(OH)_5Cl \cdot 4H_2O$	7.7−17.4	0.15−0.50	∼15−87
450	∼0.8		4.7−13.4	0.16−0.33	∼16−60

(c) time (h)	*stirring speed (rpm)*	*no. of rods measured*	*mean length (μm)*	*mean width (μm)*	*mean aspect ratio*
21	300	73	10 ± 4	0.2 ± 0.1	55 ± 31
48	300	64	12 ± 5	0.3 ± 0.1	42 ± 27
72	300	13	16 ± 8	0.4 ± 0.2	45 ± 22
48	450	50	7 ± 3	0.17 ± 0.0	46 ± 28

[a] Aging time: 48 h and temp: ∼25 °C. [b] ND: not determined.

are slightly more soluble as compared to MC−MgO.[48b,53] This has been indicated by a very rapid rise of pH from about 6 to 12 when NC−MgO is dissolved in water when compared to MC−MgO.[48b] In the present study, the relatively more rapid solubility and the higher reactivity of NC−MgO help in quickly establishing a high concentration of small nucleation sites, which subsequently aids the formation of $Mg_x(OH)_yCl_z \cdot nH_2O$ nanorods with a higher aspect ratio. The formation of gels at higher aging temperatures (50 and 70 °C), in the case of NC−MgO−II (see Table 2), is also attributed to its higher solubility/reactivity as compared to the other two oxides (NC−MgO−I and MC−MgO).

Conversion of the $Mg_x(OH)_yCl_z \cdot nH_2O$ Nanorods into $Mg(OH)_2$ Nanorods. During the conversion of the $Mg_x(OH)_yCl_z \cdot nH_2O$ nanorods into the $Mg(OH)_2$ phase, there was a structural change from triclinic to hexagonal with the elimination of water.[19a] The $Mg_x(OH)_yCl_z \cdot nH_2O$ nanorods

(53) Personal communication with Dr. J. Pickrell, Division of Toxicology, Kansas State University, Manhattan, KS.

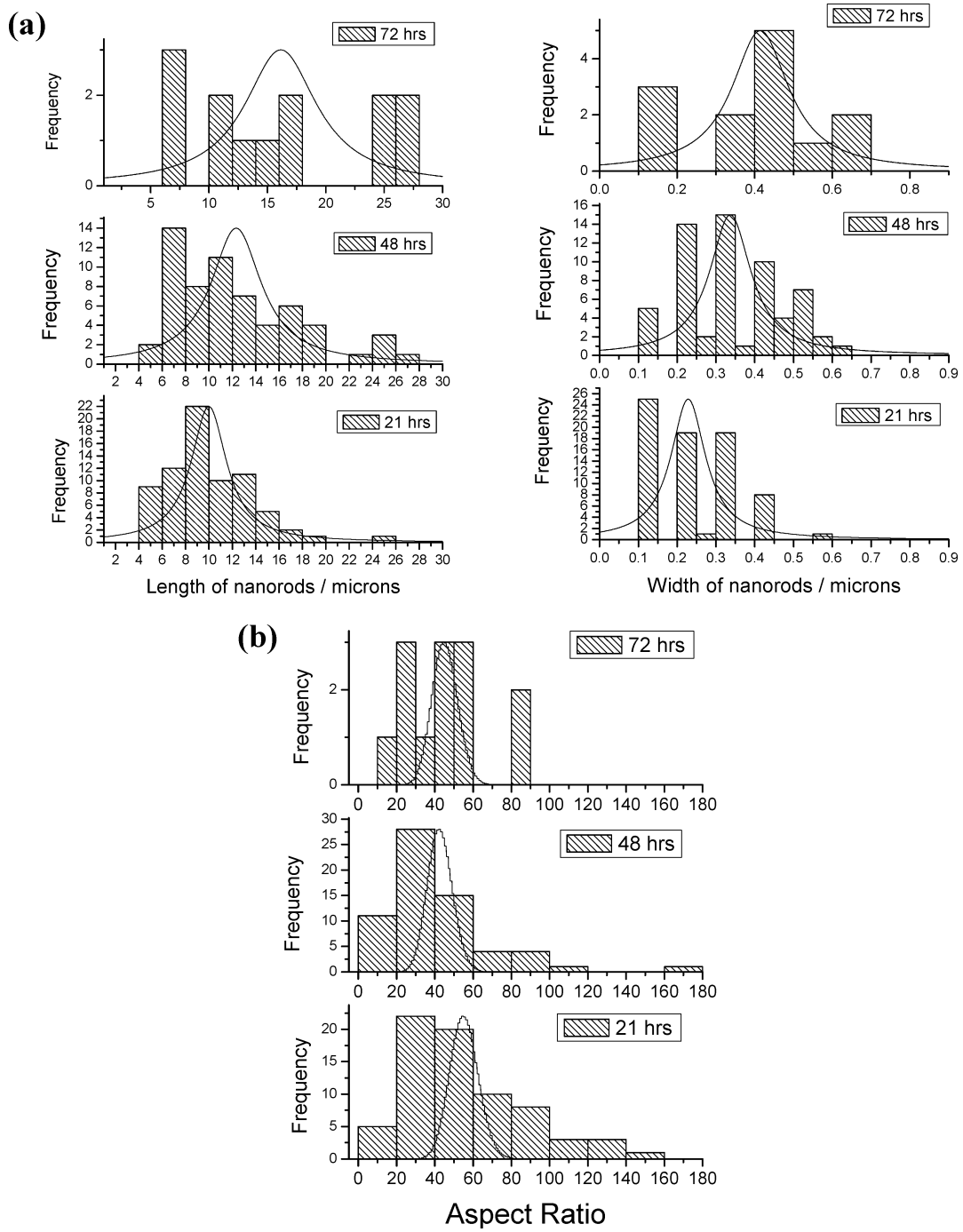

Figure 5. (a) Length and width distribution and (b) aspect ratio distribution of $Mg_3(OH)_5Cl{\cdot}4H_2O$ nanorods prepared at 300 rpm.

were converted into $Mg(OH)_2$ nanorods by NaOH treatment, and the details are as follows.

First, the oxychloride rods prepared using MC−MgO were converted into the $Mg(OH)_2$ phase by 2 M NaOH treatment at 65 °C for 3 h. Although the XRD patterns for the products (Figure 6a), obtained after NaOH treatment of $Mg_x(OH)_y$-$Cl_z{\cdot}nH_2O$, indicated $Mg(OH)_2$ rods as the major product (length: 4−12 μm and width: 100−200 nm), the TEM images (Figure 7a) always indicated the presence of smaller rods (length: ∼100−200 nm). To minimize the formation of smaller $Mg(OH)_2$ nanorods, various NaOH treatment conditions were tried; keeping the same concentration and temperature (e.g., 2 M NaOH and 65 °C), the treatment for longer times (6, 8, or 40 h) was not helpful. However, the NaOH treatment at a higher concentration at the same temperature (e.g., 4 M NaOH, 65 °C, 3 h) resulted in a larger number of lengthier nanorods (length: 4−12 μm and width: 100−200 nm) with fewer smaller rods (Figure 7b).

The use of $Mg_x(OH)_yCl_z{\cdot}nH_2O$ nanorods obtained from NC−MgO−II for the NaOH treatment would result in lengthier $Mg(OH)_2$ nanorods because of lengthier precursor rods with which (length: ≥20 μm) to begin. The $Mg_x(OH)_y$-$Cl_z{\cdot}nH_2O$ obtained from NC−MgO−II could not survive the same alkali treatment conditions used for the oxychlorides obtained from MC−MgO (e.g., 2 M NaOH, 65 °C, 3 h or 4 M NaOH, 65 °C, 3 h). The lengthier $Mg_x(OH)_yCl_z{\cdot}nH_2O$ nanorods from NC−MgO−II were attacked easily by NaOH under these conditions, and the rod structure was ruptured.

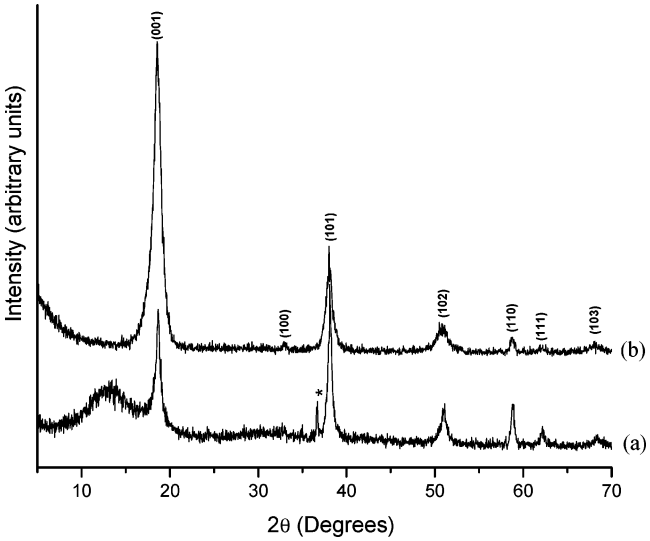

Figure 6. Typical XRD patterns of $Mg(OH)_2$ nanorods obtained from $Mg_x(OH)_yCl_z{\cdot}nH_2O$ prepared using (a) MC−MgO and (b) NC−MgO−I.

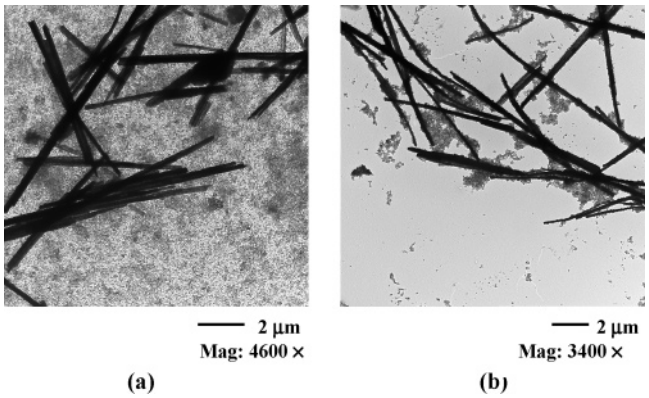

Figure 7. TEM images of $Mg(OH)_2$ nanorods obtained by NaOH treatment of the $Mg_x(OH)_yCl_z{\cdot}nH_2O$ nanorods (synthesized using MC−MgO): (a) 2 M NaOH, 65 °C, 3 h and (b) 4 M NaOH, 65 °C, 3 h.

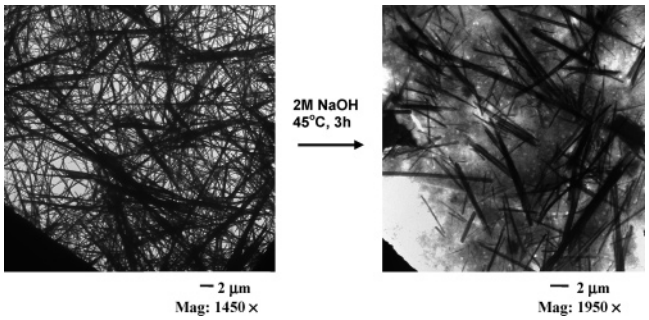

Figure 8. TEM image of $Mg(OH)_2$ nanorods obtained using $Mg_x(OH)_yCl_z{\cdot}nH_2O$ nanorods, synthesized using NC−MgO−II, with NaOH treatment condition 5, as listed in Table 5a.

Milder alkali treatment conditions by varying the concentration of NaOH, temperature, and time period of treatment were then tried (Table 5a) and optimized for the conversion of the precursor $Mg_x(OH)_yCl_z{\cdot}nH_2O$ nanorods to $Mg(OH)_2$ nanorods. The precursor ($Mg_x(OH)_yCl_z{\cdot}nH_2O$) obtained at 50 °C aging temperature (see Figure 3a) was used for the $Mg(OH)_2$ conversion.

Out of the 13 different NaOH treatment conditions, only a few (5, 6, 10, and 11 in Table 5a) yielded $Mg(OH)_2$ nanorods. A typical TEM image obtained for the $Mg(OH)_2$ nanorods is shown in Figure 8. Other conditions (1−4, 7−9, 12, and 13) yielded either irregularly shaped $Mg(OH)_2$ particles or a few $Mg(OH)_2$ rods. The length of the $Mg(OH)_2$ nanorods was found to be always shorter (2−14 μm) than that of the starting oxychloride precursor (length: ∼20 μm). Also, smaller $Mg(OH)_2$ nanorods (length: <0.2 μm) can be noticed in Figure 8. To avoid the presence of smaller $Mg(OH)_2$ nanorods, a new set of alkali treatment conditions was tried (Table 5b) with emphasis on moderate temperatures, coupled with low and high NaOH concentrations. Out of the four new conditions tried, two of them yielded $Mg(OH)_2$ nanorods without the presence of shorter $Mg(OH)_2$ nanorods, and they are (i) 1 M NaOH, 45 °C, 3 h and (ii) 4 M NaOH, 45 °C, 7 h. The former condition produced $Mg(OH)_2$ nanorods with a length of 8−15 μm and width of 200−400 nm, while the latter condition yielded $Mg(OH)_2$ nanorods with a length of 6−11 μm and width of 100−300 nm (Figure 9). The problem of the existence of smaller $Mg(OH)_2$ nanorods (compare Figures 7−9) along with longer nanorods now has been solved, and these two conditions are the best, found in the present study, to synthesize $Mg(OH)_2$ nanorods with high aspect ratios (∼40−60).

A comparison of $Mg(OH)_2$ nanorods synthesized by the present method with those reported in the literature will be

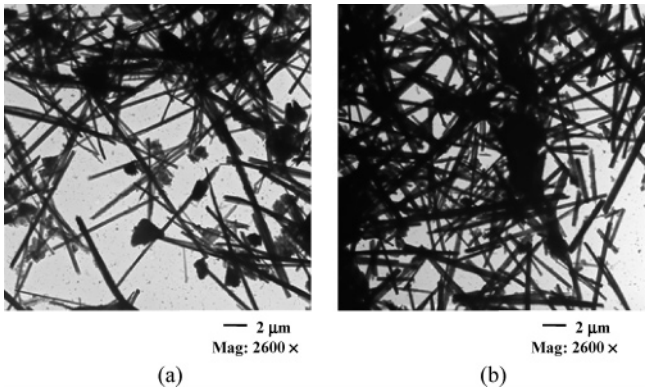

Figure 9. TEM images of $Mg(OH)_2$ nanorods obtained by NaOH treatment of $Mg_x(OH)_yCl_z{\cdot}nH_2O$ nanorods synthesized using NC−MgO−II: (a) 1 M NaOH, 45 °C, 3 h and (b) 4 M NaOH, 45 °C, 7 h.

Table 5. (a) Various NaOH Treatment Conditions Employed for Conversion of the Oxychloride Precursor[a] to $Mg(OH)_2$ Nanorods and (b) Improved NaOH Treatment Conditions Employed for Conversion of the Oxychloride Precursor[b] to $Mg(OH)_2$ Nanorods

(a)	NaOH treatment conditions	TEM observation
1	2 M NaOH(EtOH-H_2O), 70 °C, 3 h	no rods
2	4 M NaOH(EtOH-H_2O), 70 °C, 3 h	no rods
3	4 M NaOH(EtOH-H_2O), 70 °C, 6 h	no rods
4	4 M NaOH(EtOH-H_2O), 70 °C, 19 h	no rods
5	2 M NaOH(EtOH-H_2O), 45 °C, 3 h	length: ∼4−12 μm
6	4 M NaOH(EtOH-H_2O), 45 °C, 3 h	length: ∼4−14 μm
7	1 M NaOH(EtOH-H_2O), 25 °*C (RT), 3 h*	no rods
8	2 M NaOH(EtOH-H_2O), 25 °C, 3 h	no rods
9	4 M NaOH(EtOH-H_2O), 25 °C, 3 h	no rods
10	4.5 M NaOH(EtOH-H_2O), 25 °C, 3 h	length: ∼2−8 μm
11	6 M NaOH(EtOH-H_2O), 25 °C, 3 h	length: ∼4−8 μm
12	2 M NaOH(H_2O), 25 °C, 3 h	no rods
13	6 M NaOH (H_2O), 25 °C, 3 h	no rods

(b)	NaOH treatment conditions
1	1 M NaOH (EtOH-H_2O), 45 °C, 3 h
2	1 M NaOH (EtOH-H_2O), 45 °C, 6 h
3	2 M NaOH (EtOH-H_2O), 45 °*C, 6 h*
4	4 M NaOH (EtOH-H_2O), 45 °*C, 7 h*

[a] Prepared using NC−MgO−II. [b] Obtained using NC−MgO−II.

Table 6. Summary of Reported Dimensions of Mg(OH)$_2$ Nanorods from the Literature

ref	dimensions of nanorods	synthesis method
19a	length: 10 μm or longer width: 40−200 nm	precursor approach
42	length: several micrometers width: ∼200 nm	solvothermal synthesis
43	length: 200−400 nm width: 8−20 nm	solvothermal synthesis
44	length: ∼3 μm width: ∼30 nm	hydrothermal synthesis
45	length: >250 nm width: 8−10 nm	liquid−solid arc discharge method
46	length: ∼4 μm width: ∼95 nm	homogeneous precipitation
present study	length: ∼8−15 μm width: ∼200−400 nm	precursor approach

worthwhile. The various reported methods for the synthesis of Mg(OH)$_2$ nanorods is summarized in Table 6. Mg(OH)$_2$ nanorods with lengths varying from about 0.2 to 10 μm or more and diameters varying from 30 to 400 nm have been synthesized by various groups. Out of the reported methods, the procedure by Lieber and Wei[19a] has a similar approach of the present study, but there are significant differences when compared with the present study: (i) the precursor nanorods (Mg$_x$(OH)$_y$Cl$_z$·nH$_2$O) can be synthesized at room temperature within about 21 h in the present study. Lieber and Wei's process takes about 48 h to synthesize the precursor nanorods. The reduction in time for the synthesis of precursor rods is significant, and it is helpful for the subsequent synthesis of Mg(OH)$_2$ nanorods, (ii) the effect of the crystallite size of MgO used during the synthesis of precursor nanorods has been investigated for the first time in the present study, and this has not been studied by Lieber and Wei. The crystallite size of MgO (NC vs MC) has a profound effect on the chemical composition and morphology of the Mg$_x$(OH)$_y$Cl$_z$·nH$_2$O nanorods synthesized. The study, for the first time, provides in-depth details of methods for producing Mg$_x$(OH)$_y$Cl$_z$·nH$_2$O and Mg(OH)$_2$ nanorods.

Conclusion

Mg(OH)$_2$ nanorods were synthesized starting from a precursor, Mg$_x$(OH)$_y$Cl$_z$·nH$_2$O. The Mg$_x$(OH)$_y$Cl$_z$·nH$_2$O nanorods were first synthesized from MgCl$_2$·6H$_2$O and MgO under aqueous conditions. The effect of various parameters such as aging time, aging temperature, nature of MgO (NC vs MC), stirring speed, and concentration of reagents were investigated during the synthesis of the Mg$_x$(OH)$_y$Cl$_z$·nH$_2$O nanorods. Among these parameters, the nature of MgO has a profound effect on the Mg$_x$(OH)$_y$Cl$_z$·nH$_2$O rods formed. Under ambient aging conditions, only using NC−MgO leads to the complete formation of precursor nanorods. NC−MgO yielded longer and thinner precursor rods (length: ≥20 μm and width: ∼170 nm), while MC−MgO yielded shorter (length: few micrometers and width: 0.1−0.4 μm). Mg$_x$(OH)$_y$Cl$_z$·nH$_2$O nanorods with higher aspect ratios (∼60−90) could be synthesized using NC−MgO. The formation mechanism of the Mg$_x$(OH)$_y$Cl$_z$·nH$_2$O nanorods was also studied. MgO is very important for the formation of the Mg$_x$(OH)$_y$Cl$_z$·nH$_2$O nanorods, and a seed mediated growth mechanism was ruled out. The higher surface area and reactivity of NC−MgO in comparison with MC−MgO allows the rapid formation of nucleation sites in large numbers that subsequently grow into thin Mg$_x$(OH)$_y$Cl$_z$·nH$_2$O nanorods.

The precursor Mg$_x$(OH)$_y$Cl$_z$·nH$_2$O nanorods were converted into Mg(OH)$_2$ nanorods by NaOH treatment. The conversion conditions were optimized with respect to the concentration of NaOH, solvent used, treatment time, and temperature. Mg$_x$(OH)$_y$Cl$_z$·nH$_2$O nanorods prepared using MC−MgO yielded, in addition to longer Mg(OH)$_2$ nanorods (4−12 μm), shorter Mg(OH)$_2$ nanorods (length: <100 nm). On the other hand, Mg$_x$(OH)$_y$Cl$_z$·nH$_2$O nanorods prepared using NC−MgO yielded the longest Mg(OH)$_2$ nanorods (8−15 μm) with shorter rods absent. Mg(OH)$_2$ nanorods with aspect ratios ∼40−60 could be synthesized this way. A comparison of the present method with the reported methods indicates that the present one is a faster way of synthesizing the precursor (Mg$_x$(OH)$_y$Cl$_z$·nH$_2$O) rods followed by their conversion into Mg(OH)$_2$ nanorods.

Acknowledgment. This work was partially funded through the award of a contract from the United States Marine Corps Systems Command to M2 Technologies Inc., KY. We thank the Kansas State University Biology Research Microscope and Image Processing Facility, which has been supported in part by the NSF EPSCoR Program, by the NASA EPSCoR Program, by University resources, and by the Kansas Agricultural Experiment Station. Thanks are also due to the NanoScale Corporation for providing the nanocrystalline metal oxides.

CM070666T